Original Article

Journal of Intelligent Material Systems and Structures

Journal of Intelligent Material Systems and Structures
1–12

DOI: 10.1177/1045389X17705210
journals.sagepub.com/home/jim
SAGE

Quantitative and qualitative analyses of mechanical behavior and dimensional stability of styrene-based shape memory composites

Wessam Al Azzawi[1,2], Mainul M Islam[1], Jinsong Leng[3,4], Fengfeng Li[3] and Jayantha A Epaarachchi[1]

Abstract

The effect of glass fiber reinforcement on the mechanical properties and geometrical shape stability during the thermomechanical cycle of the shape memory polymer composite has been investigated. A substantial improvement in the mechanical properties due to glass fiber reinforcement has been realized. However, unexpected deformation has been observed during heating process, particularly in the first thermomechanical cycle. This unanticipated deformation negatively affects the geometrical shape stability of the composite, and as a consequence the geometry preciseness of the structural parts manufactured with shape memory polymer composites will be reduced. In this article, the unanticipated thermal deformation in the shape memory polymer composites during the heating has been observed experimentally, and constitutive relationships to describe this behavior have been developed. Furthermore, an application of a constant tensile load during the heating process on the shape memory polymer composite part was found to be a reliable solution to reduce the thermal distortion effect and improve the geometric stability of the composite. The results showed that developed constitutive relations have shown a good agreement with the experimental results. Furthermore, the proposed applied tensile load has shown significant improvement in the shape memory polymer composite samples' geometrical shape stability when subjected to a temperature increase.

Keywords

Shape memory polymers, composites, thermomechanical analysis, modeling

Introduction

At present, shape memory polymers (SMPs) are being evolved intensely and represent a fast growing branch of smart materials' research. The SMPs have a fascinating capability of keeping a temporary shape and subsequently recovering the original shape on exposure to a particular external stimulus. Since the discovery of the SMPs in 1980s, the global research interest in these materials has been rapidly growing (Beloshenko et al., 2005; Gunes and Jana, 2008; Lendlein and Kelch, 2002; Liu et al., 2009), because of their inimitable advantages of good manufacturability, high shape deformability, large recoverability, good biodegradability, and an easily tailorable glass transition temperature (T_g) (Lendlein and Kelch, 2002; Leng et al., 2011; Ohki et al., 2004). These advantages make the SMPs very competitive materials to replace the shape memory alloys (SMAs), which are known to have good mechanical properties, are relatively expensive to manufacture (DesRoches and Smith, 2004), and have relatively high density.

As a stimuli-responsive material, SMPs have a large number of stimuli such as magnetic field (Schmidt, 2006), electrical field (Sahoo et al., 2005), heat (Ji et al., 2006), light (Lendlein et al., 2005), moisture (Yang et al., 2005), and change in the pH value (Han et al., 2012). Among these types, heat is the most common triggering mechanism and it represents the underlying principle for some of the other types.

[1]Center for Future Materials, Faculty of Health, Engineering and Sciences, University of Southern Queensland, Toowoomba, QLD, Australia
[2]College of Engineering, University of Diyala, Baqubah, Iraq
[3]Department of Astronautical Science and Mechanics, Harbin Institute of Technology (HIT), Harbin, China
[4]Centre of Composite Materials and Structures, Harbin Institute of Technology (HIT), Harbin, China

Corresponding author:
Jayantha A Epaarachchi, Centre for Future Materials, Faculty of Health, Engineering and Sciences, University of Southern Queensland, West Street, Toowoomba, QLD 4350, Australia.
Email: Jayantha.Epaarachchi@usq.edu.au

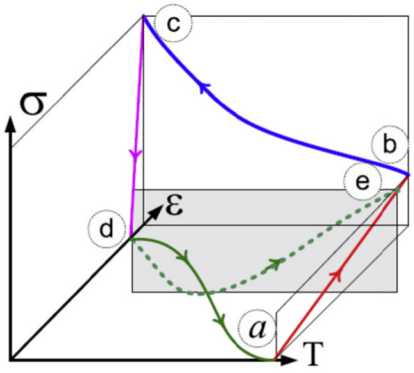

Figure 1. Typical temperature–stress–strain diagram illustrating the thermomechanical behavior of the SMP (Baghani et al., 2014).

The typical thermomechanical cycle of the SMP is shown in Figure 1. The cycle starts at point (a) where the material in rubbery phase is deformed under external load. The achieved strain at (b) is held constant and cooled down to point (c). At this point, the material is released from the external constraint, the stress fades to zero, and the strain slightly changes to point (d). Point (d) signifies the temporary shape, and (a–b–c–d) path denotes the shape programming part of the cycle. The next sequence of the thermomechanical cycle is the shape recovery part, which starts at point (d) when the material is triggered by heat and ends at (a) where the original shape is recovered. Path (d–a) is termed as stress-free strain recovery process, since it takes place under no constrains. However, another type of recovery can be achieved if the material is heated under a constrained strain. This type of recovery is denoted as fixed-strain stress recovery, and the stress evolved inside the material is denoted by point (e).

SMPs have relatively low stiffness, and therefore many types of reinforcements and fillers have been used to improve their mechanical properties (Nishikawa et al., 2012). The reinforcing materials are ranging from particles, such as carbon black (Liu et al., 2009), to short or continuous fibers (e.g. glass fibers; Ivens et al., 2011) and carbon fibers (Lu et al., 2010). However, shape memory polymer composites (SMPCs) reinforced with particles and fibers have distinct material properties. The continuous fiber–reinforced SMPCs demonstrate higher mechanical properties (Abrahamson et al., 2003; Lan et al., 2009), while particles and short fiber–reinforced SMPCs show significant improvement in electrical and thermal conductivity and magnetic-responsive performance (Leng et al., 2007; Liu et al., 2009; Sahoo et al., 2007).

In general, composites are made up of constituents that have different mechanical properties, and consequently the general properties of the SMPCs are varying within the limits of constituent materials. In some cases, the properties of constituent materials take the control of the structural and thermal characteristics of SMPCs such as uneven thermal expansion of the fiber and SMP matrix which leads to a differential thermal strain between the fiber and the matrix (Nairn and Zoller, 1985). During the SMPC curing process, the SMP resin solidifies at curing temperature from the melt to solid state, bonds firmly to the included fibers, and constrains the fibers' thermal strain. When SMPC has cooled down to room temperature at the end of the curing process, the different thermal expansion behaviors of fiber and matrix have caused a residual stress at the interface (Vedula et al., 1988). Consequently, interfacial reaction transmits various morphological modification to the matrix in proximate to the fiber (Ray, 2004). This unpredicted shape deformation in the SMPC will cause significant changes in the geometry of SMPC parts during the thermomechanical cycle of the SMPC.

In recent years, fiber-reinforced SMPCs have made inroads to a wider range of structural applications including but not limited to aerospace (Lan et al., 2009; Leng et al., 2011; Keller et al., 2004) where SMPC components were designed as driving devices and replaced the traditional mechanical systems (Liu et al., 2014). Consequently, the SMPC parts are required to be within the designed geometrical dimensions, and therefore the deformation caused by the fiber during the thermomechanical cycle should be carefully considered.

The effects of glass fiber reinforcement on the mechanical properties and geometry disfigurement, during the thermomechanical cycle, have been studied in this research. Geometric disfigurement of the SMPCs during heating is attributed to the slump in matrix mechanical properties which allows releasing the fibers' thermal strain trapped inside the composite during curing process. Many literatures have pointed this effect in the general fiber-reinforced composites and considered the disparity in expansion coefficient between the matrix and the fibers (Hahn, 1976; Manders and Bader, 1981). However, for SMPCs, this effect is more dominate due to the considerable reduction in stiffness of SMP matrix when heated above T_g. Therefore, in this research, the effect of fibers on the SMPC shape deformation has been experimentally and analytically investigated. In experimental part, dynamic and thermomechanical analyses have been employed to characterize the material properties and thermal deformation behavior. Furthermore, a few analytical relations have been formulated into a model that describes the effect of the fibers on the geometrical shape stability when the SMPC undergoes heating process.

Materials and experimental methods

The styrene-based SMP type C, which was supplied by Harbin Institute of Technology, China, has been used

Table 1. Operation mode, purpose, clamping type, frequency and temperature setting for the dynamic mechanical analysis to investigate the thermal and mechanical properties of the SMP and SMPC samples.

Mode of operation	Purpose	DMA clamp type		Frequency (Hz)	Temperature
Frequency mode	T_g Storage modulus	Dual cantilever		1	Ramp at 10°C/min from 30°C to 115°C
TMA mode	Thermal expansion behavior	Tensile	Free Constrained (0.5 MPa)	–	Ramp at 1°C/min
Controlled force mode	Mechanical properties	Tensile		–	35°C 55°C 75°C 95°C

DMA: dynamic mechanical analysis; TMA: thermal mechanical analysis.

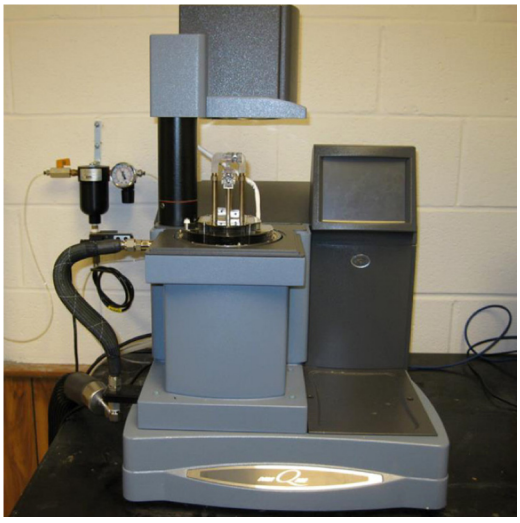

Figure 2. DMA Q800 instrument used in different operation modes and different sample clamp arrangements.

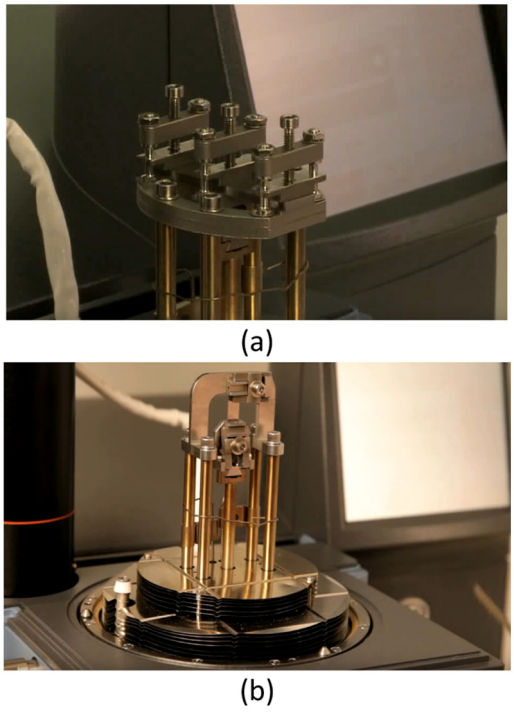

Figure 3. DMA clamp arrangements for (a) dual cantilever frequency mode and (b) tensile test for TMA and controlled force modes.

to prepare the samples. Two different SMPCs with 20% and 25% by weight of woven glass fiber AR177100 W/C 450 0/90 (supplied by Colan Australia) were produced, respectively. A rectangular glass mold coated with thin film of Teflon has been used to cast the specimens. The curing process has been done in a temperature-controlled oven, at 85°C for 24 h.

A TA instrument dynamic mechanical analyzer (DMA Q800) shown in Figure 2 has been used in three different operating modes to investigate the thermal and mechanical properties of both SMP and SMPC samples as shown in Table 1. The frequency mode has been used to identify the materials' glass transition temperatures (T_g) and to characterize the storage modulus. The frequency of 1 Hz and temperature ramp of 10°C/min have been selected to scan the material over a temperature span from 30°C to 115°C. The dual cantilever bending arrangement as shown in Figure 3(a) has been used, with the specimens' size of 35 mm × 14 mm × 1.5 mm. The T_gs of the SMP and SMPC samples have been measured initially using the storage modulus–temperature relation. An innovative idea of temperature derivative of the storage modulus–temperature relation, proposed by Zhou et al. (2009), has been implemented to locate T_gs.

The thermal strains in SMP and its composites are significant during the operational temperature fluctuation. Liu et al. (2003) have shown that the thermal strain caused by the thermomechanical cycles will result in extremely complex strain field inside the material. Therefore, thermal expansion behaviors of the SMPCs have been investigated experimentally and analytically. DMA Q800 in thermal mechanical analysis (TMA)

mode has been used to observe the thermal expansion behavior of the specimens. The thermal strain was acquired using tension test while the temperature was increasing at a constant rate. Two different testing methods have been employed in this testing mode. In the first method, the specimens were allowed to thermal expand at free condition (i.e. under no tensile/compression load) while the temperature is ramping. This case is similar to heating process encountered in the shape programming part of the thermomechanical cycle. In the second method, a constant tensile stress of 0.5 MPa was applied on the specimens while the temperature is ramping. The purpose of this method is to investigate the thermal strain behavior under constrains, which is the case that happens in the shape recovery part of the SMP thermomechanical cycle. In both methods, the thermal strain has been monitored while the temperature is ramping at 1°C/min.

The controlled force mode has also been selected to examine the effect of fiber reinforcement on the mechanical properties of the SMPC specimens (10.5 mm × 6.5 mm × 1.5 mm). The test has been done at different temperatures to investigate the temperature effect on the mechanical properties. A tension test was used, as shown in Figure 3(b), where the tensile load was ramping isothermally, at four selected temperatures, 35°C, 55°C, 75°C, and 95°C, which covers the glassy phase, rubbery phases, and the transition region of the SMP.

Development of empirical constitutive equations for thermal strain behavior of SMPC

Liu et al. (2006) have developed a constitutive model for SMP, which consists of internal state variables based on the experimental results and the molecular mechanism of the shape memory effect of SMP. According to this model, there are two kinds of extreme phases; glass and rubber exist in SMP at an arbitrary temperature. Accordingly, the SMP is assumed here to be the mixture of these two interchangeable phases, and they are transferable to each other through the external heat stimuli. The volume fraction for each phase in the polymer matrix can be defined as (Tan et al., 2014)

$$\varphi_r = \frac{V_r}{V_{matrix}}, \varphi_g = \frac{V_g}{V_{matrix}}, \varphi_r + \varphi_g = 1 \tag{1}$$

Here, V_r and V_g denote the volume of the rubbery and glassy phases in the matrix, respectively. V_{matrix} represents the total polymer matrix volume, and φ_r and φ_g stand for the rubbery and glassy phases' volume fraction, respectively.

The total strain in the SMPC, during the thermomechanical cycle, can be decomposed into two components: mechanical and thermal strains as follows (Baghani and Taheri, 2015)

$$\varepsilon = \varepsilon_m + \varepsilon_T \tag{2}$$

where ε, ε_m, and ε_T denote the SMPC total strain, mechanical strain, and thermal strain, respectively. By assuming small strains, the mixture rule in the SMPC is used, and the total strain is divided into matrix strain, fiber strain, and thermal strain (Baghani and Taheri, 2015; Xu and Li, 2010)

$$\varepsilon = (1 - \phi_f)(\varphi_r \varepsilon_r + \varphi_g \varepsilon_g + \varepsilon_s) + \phi_f \varepsilon_f + \varepsilon_T \tag{3}$$

where ε_r and ε_g are the elastic strains in the rubbery and glassy phases, respectively; ε_s denotes the strain stored and released in the SMP matrix during the cooling and heating processes; and ε_f stands for the elastic strain in the fiber. ϕ_m and ϕ_f are the matrix and fiber volume fraction, respectively, and can be defined as (Tan et al., 2014)

$$\phi_m = \frac{V_{matrix}}{V}, \phi_f = \frac{V_{fibre}}{V}, \phi_m + \phi_f = 1 \tag{4}$$

Here, V is the total composite volume; V_{matrix} and V_{fibre} are the volume of the matrix and fiber, respectively.

The thermal strain in the last part of equation (3) is constitutively defined as (Tan et al., 2014)

$$\varepsilon_T = (1 - \phi_f)\varepsilon_T^m + \phi_f \varepsilon_T^f \tag{5}$$

where ε_T denotes the thermal strains, and m and f in the superscript represent the matrix and fibers, respectively. Since the matrix is presumed to be a mixture of two phases, the thermal strain in the polymer is calculated by adding the thermal strain in these two phases as

$$\varepsilon_T^m = \int_{T_o}^{T} \left[\left(1 - \varphi_g(T)\right)\alpha_r + \varphi_g(T)\alpha_g\right] dT \tag{6}$$

Here, α_r and α_g are the thermal expansion coefficients in the rubbery and glassy phases of the matrix, respectively. T_o and T represent the initial and final temperatures of the heating process, respectively. By substituting equation (6) into equation (5), we get

$$\varepsilon_T = (1 - \phi_f) \int_{T_o}^{T} \left[\left(1 - \varphi_g(T)\right)\alpha_r + \varphi_g(T)\alpha_g\right] dT + \phi_f \int_{T_o}^{T} \alpha_f dT \tag{7}$$

Equation (7) describes the thermal strain in the SMPC, where ϕ_f and α_f represent the non-temperature-dependent fiber volume fraction and thermal expansion coefficient, respectively. By resubmitting

Table 2. Material parameters.

Material parameter	Value			Units
E_f, E_g, E_r	8×10^3, 1500, 180			MPa
α_f, α_g, α_r	5×10^{-6}, 1.3×10^{-4}, 1.3×10^{-3}			1/°C
	SMP	20% SMPC	25% SMPC	
T_g	76	82	86	°C
T_l	56	62	66	
T_h	96	102	106	
$_g(T)$	$\frac{\tanh((T_h - T_g)/b) - \tanh((T - T_g)/b)}{\tanh((T_h - T_g)/b) - \tanh((T_l - T_g)/b)}, b = 11.34$			

SMP: shape memory polymer; SMPC: shape memory polymer composite.

equation (7) in equation (3), a complete expression for strain in SMPC can be achieved as

$$\begin{aligned}\varepsilon = {} & (1-\phi_f)(\varphi_r\varepsilon_r + \varphi_g\varepsilon_g + \varepsilon_s) + \phi_f\varepsilon_f \\ & + (1-\phi_f)\int_{T_o}^{T}\left[\left(1-\varphi_g(T)\right)\alpha_r + \varphi_g(T)\alpha_g\right]dT \\ & + \phi_f\int_{T_o}^{T}\alpha_f dT\end{aligned} \tag{8}$$

Modeling of "free of load" thermal strain behavior

When the matrix solidifies at curing temperature, its stiffness increases significantly due to conversion from viscous to solid state. Consequently, the matrix traps the thermal strain occurred in the fibers at the curing temperature and retains the fibers under tension and matrix under compression. By assuming perfect bonding between the fibers and matrix, the thermally induced tensile stress in the fibers generates a compression strain in the SMPC which can be described as

$$\varepsilon_T^c = \phi_f\frac{E_f}{E_c(T)}\alpha_f(T_{curing} - T) \tag{9}$$

where ε_T^c is the thermal compression strain in the composite, $E_c(T)$ is the temperature-dependent modulus of the composite, and E_f is the modulus of the fiber. Here, E_f is considered to be invariant with temperature because its variation is negligible comparing to the matrix modulus over the temperature range (25°C–120°C) under consideration. $E_c(T)$ is calculated from the rule of mixture (10)

$$E_c(T) = \left[\frac{\phi_f}{E_f} + \frac{(1-\phi_f)}{E_m(T)}\right]^{-1} \tag{10}$$

Then using the modulus of the glassy and rubbery phases (E_g, E_r) and the glass volume fraction $\varphi_g(T)$ shown in Figure 4, the temperature-dependent modulus of the matrix has been calculated using equation (11) (Baghani et al., 2014)

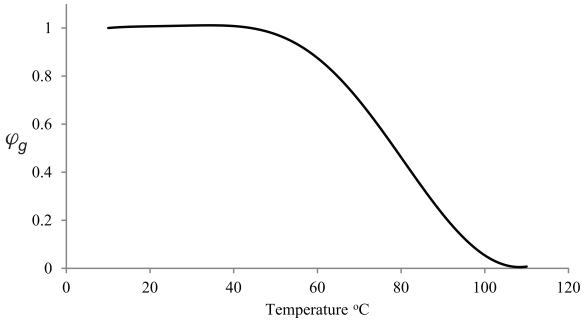

Figure 4. Glass volume fraction–temperature relation of the styrene-based shape memory polymer.

$$E_m(T) = \left[\frac{\varphi_g(T)}{E_g} + \frac{\left(1-\varphi_g(T)\right)}{E_r}\right]^{-1} \tag{11}$$

All material parameters used in the analysis are reported in Table 2.

When the SMPC is heated above the room temperature, the temperature difference in equation (9) reduces. As a result, the compressive strain on the SMPC caused by the fibers will be reduced. Moreover, due to heating, a thermal expansion takes place in the matrix itself and an expansion happens in the composite which can be described by adding matrix thermal expansion to equation (9)

$$\varepsilon^c = \varepsilon_T^c + \alpha_m(T)\Delta T \tag{12}$$

Here, ε^c represents the thermal strain in the composite, and $\alpha_m(T)$ is the expansion coefficient of the matrix which is temperature-dependent and can be calculated from the glass and rubber phases' expansion coefficient using the rule of mixture. ΔT represents the temperature variation. However, when the temperature increases, a considerable drop in $E_m(T)$ takes place, and the compressive stress in fibers will dominate the process. This will cause contraction in the composite which can be described by equation (9). This equation also shows that an increase in the fiber fraction (ϕ_f) will increase the contraction of SMPC.

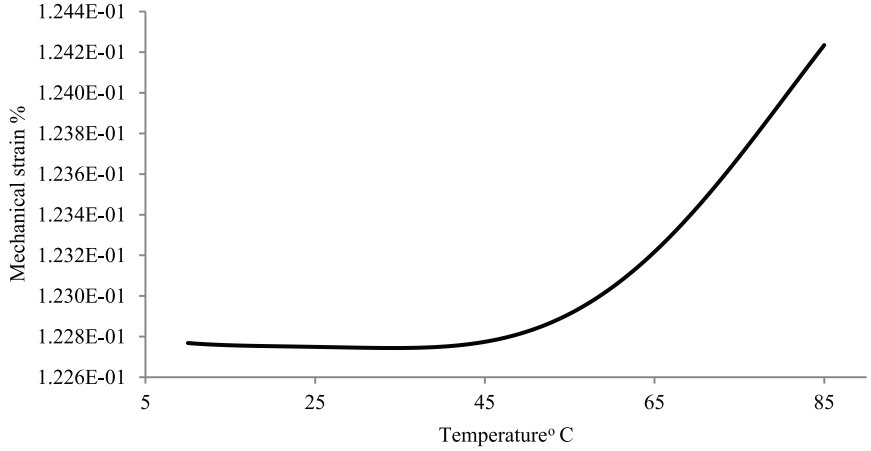

Figure 5. The temperature effect on the SMPC mechanical strain under constant stress, a considerable increase in strain at the beginning of the transition region due to the drop in the matrix modulus.

Modeling of thermal strain behavior under "applied loading"

Applying mechanical stress during the heating process will change the SMPC deformation behavior. Due to the variation in the matrix modulus with the temperature, the strain in the SMPC can be described by

$$\varepsilon_m^c = \frac{\sigma}{E_c(T)} \tag{13}$$

Here, ε_m^c represents the mechanical strain in the composite due to the applied stress (σ), and $E_c(T)$ denotes the temperature-dependent composite modulus. The mechanical strain described in equation (13) is presented in Figure 5 where considerable increase in strain can be noticed with the beginning of the transition region due to drop in the matrix modulus. Then the total strain in the composite under applied mechanical stress can be obtained by adding equations (12) and (13)

$$\varepsilon_{total} = \varepsilon_T^c + \alpha_m(T)\Delta T + \frac{\sigma}{E_c(T)} \tag{14}$$

Here, ε_{total} is the total strain in the SMPC, with the existence of external stress.

Figure 6 illustrates the flowchart that summarizes the SMPC shape stability development model. The thermal and mechanical properties of the materials (Table 2) have been given as input. Then the strains of the two cases, free thermal expansion and constrained thermal expansion, have been determined and compared to assess the shape stability improvement.

However, this model has considered only the internal stresses and the shape caused by the applied load and thermal expansion of the matrix and reinforcing fibers. At the recovery stage, the same stresses will not be generated by the material to resist any external constraint due to major differences of materials' phases in programming and recovery phases though the original shape will be recovered at the end of the process. Hence, the use of the proposed model is not recommended for calculation of shape/force recovery. An appropriate additional formulation to the present model is warranted before using it to calculate the recovery forces.

Results and discussion

The thermal and mechanical properties of styrene-based SMPs and its glass fiber–reinforced SMPCs have been experimentally investigated. Glass fiber reinforcement has significantly improved the mechanical properties of SMP. However, glass fibers have introduced an unanticipated deformation during heating process to SMP particularly in the first thermomechanical cycle. This unanticipated deformation will negatively influence SMPC parts which need critical geometrical tolerances.

Glass transition temperature T_g

Figure 7(a) and (b) depicts storage modulus, loss modulus, and tan delta of neat SMP specimen used in this research. Since the storage modulus changes considerably in the transition region ($T_l - T_h$), the storage modulus curve is more reasonable to be used to define T_g (Zhou et al., 2009). A relationship between the storage modulus and the temperature has been deduced by curve-fitting to the DMA results. This relationship was differentiated with respect to the temperature to find T_g.

Figure 8 depicts the curves of temperature derivatives of storage modulus versus temperature of neat and two SMPC samples. The temperature corresponding to the minima of the curves corresponds to the T_g for that particular sample. The T_g for neat SMP, 20%,

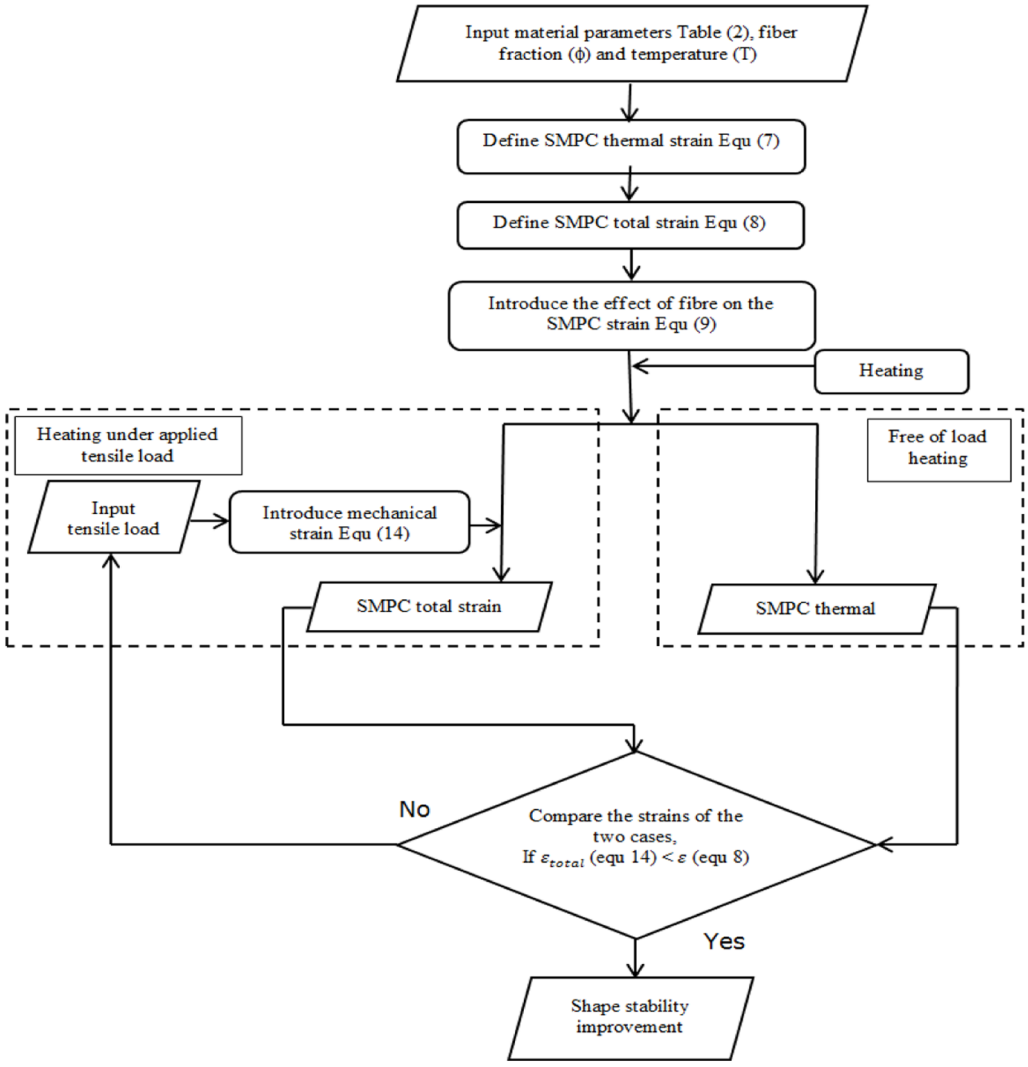

Figure 6. Flowchart for the development of the shape stability of the SMPC.

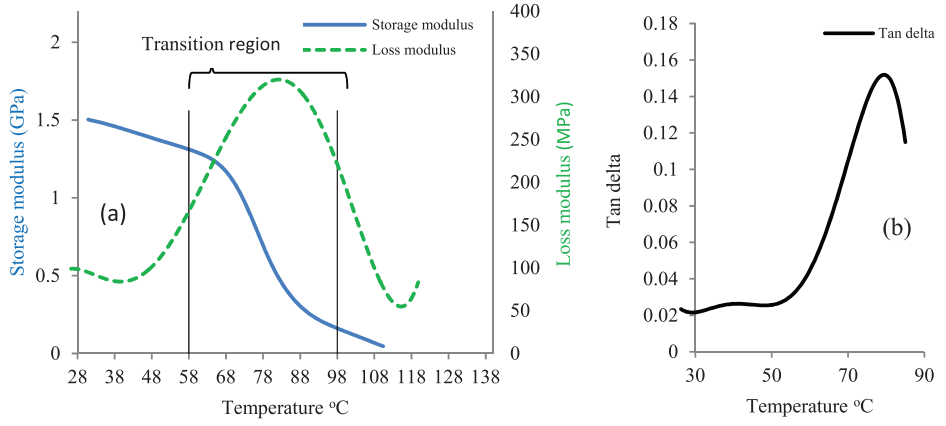

Figure 7. Dynamic mechanical analysis results of neat SMP: (a) storage modulus and loss modulus and (b) tan delta.

and 25% SMPCs has found to be 76°C, 82°C, and 86°C, respectively. It can be noticed that the minima of the curves in Figure 8 are shifting horizontally to right which indicates that T_g is increasing with the increase in fiber volume fraction. This observation can be attributed to the development of an interface in the SMPCs

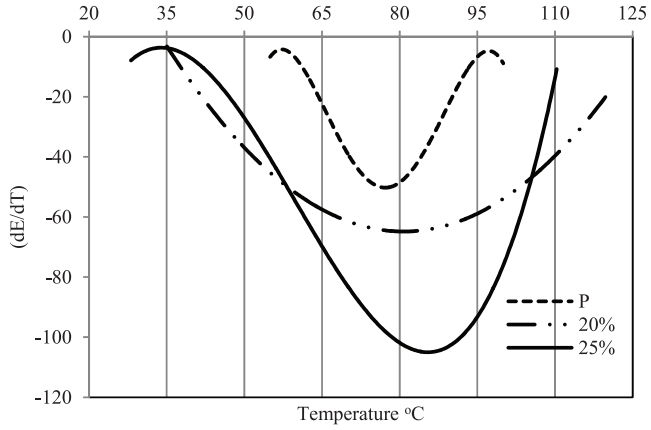

Figure 8. Temperature derivative of storage modulus–temperature relation versus temperature of neat SMP (P) and (20% and 25%) SMPCs. Minimum of the derivative curves indicates the initiation of the storage modulus drop and signposts glass transition temperature.

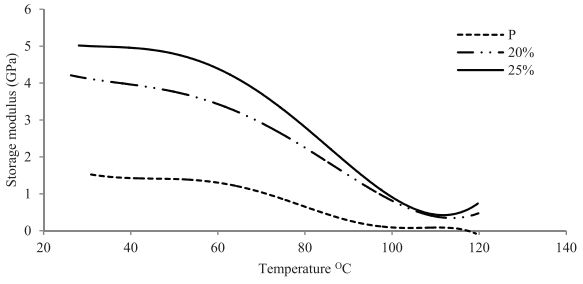

Figure 9. Temperature and fiber effects on the storage modulus of neat SMP (P) and two different SMPCs.

that impedes the heat transfer inside the matrix. Another possible explanation for the increased T_g is the thermal capacity and low thermal conductivity of the glass fiber which delays the heating and softening onset of the matrix. The same phenomenon has been reported by Lan et al. (2009). However, Razzaq and Frormann (2007) have reported a reduction in T_g for the particle filled/SMP which was due to the increase in material thermal conductivity. It has also been noticed that the storage modulus varies significantly between T_l ($= T_g - 20°C$) and T_h ($= T_g + 20°C$); however, it slightly differs below T_l and above T_h. Thus, the temperature range ($T_l - T_h$) which has been defined as the material transition region is justified.

Development of SMPC properties

Figure 9 shows the storage modulus of neat SMP and two SMPCs acquired from the frequency mode of the DMA test. All specimens show higher storage modulus at lower temperatures and critically low modulus at higher temperatures due to the entropy elasticity caused by the micro-Brownian movement in rubbery phase (Ohki et al., 2004). It is also apparent from Figure 9 that glass fiber reinforcement did not change the material behavior when heated from temperatures below to above T_g. Interestingly, all samples have shown a glassy phase followed by transition region before been changed to rubbery phase. The glass fiber has significantly improved the storage modulus as anticipated; however, the improvement has been found to be temperature-dependent. When the fiber fraction increased from 20% to 25%, the storage modulus increased by 25% below T_g. However, above T_g, the increase in the modulus is almost half of the below T_g modulus. This implies that the effect of fiber reinforcement dominates at lower temperature, because the applied load has been evenly distributed through SMPC. However, at higher temperatures, matrix modulus degrades and polymers become pliable and lose its homogeneous behavior, thus the mechanical properties of the composite have considerably decreased. Figure 9 also shows that the storage modulus of the SMP has dropped by 85% comparing to 75% for the SMPCs during the transition from glassy to rubbery phases. Accordingly, the fiber has reduced the difference in between the glassy and rubbery moduli, which is good from the structural point of view; however, this can negatively affect the shape fixity of the SMPC (Fejős et al., 2012; Ratna and Karger-Kocsis, 2008).

The stiffness of SMP is continuously varying during the thermomechanical cycle, and it considerably decreases at the elevated temperatures. Different fiber volume fraction samples have been tested at different temperatures, 35°C, 55°C, 75°C, and 95°C, to investigate the fiber influence on the stiffness development at each temperature level. For this test, the control force mode of operation has been adopted on the DMA, and 18 N tensile load and 0.35×10^{-6} m/min displacement rate were set. The temperatures were individually set up for each level.

The stiffness of neat SMP, 20%, and 25% SMPCs is presented in Figures 10 to 12, respectively. Figure 10

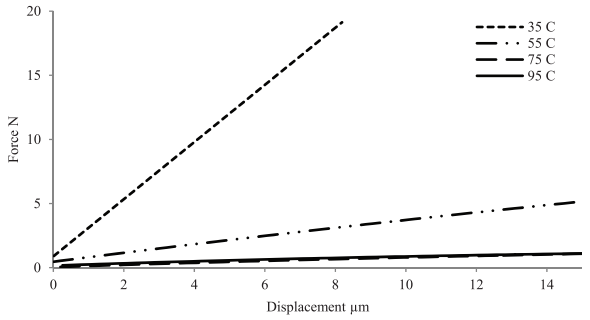

Figure 10. Force–displacement diagram illustrating thermomechanical behavior of neat shape memory polymer at different temperatures.

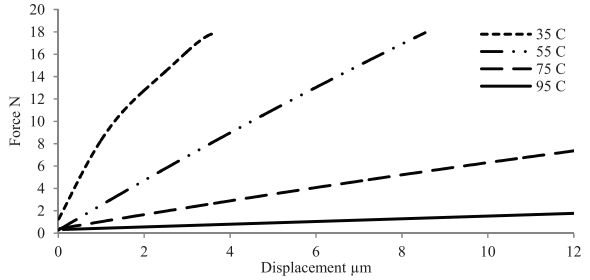

Figure 11. Force–displacement diagram illustrating thermomechanical behavior of (20%) fiber fraction shape memory polymer composites at different temperatures.

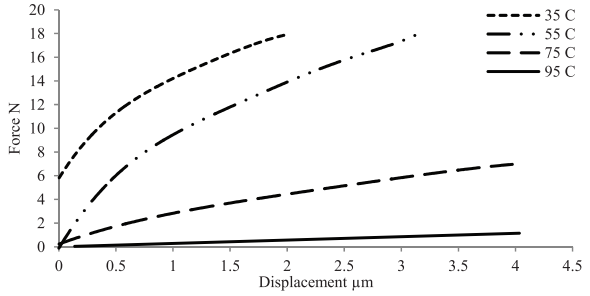

Figure 12. Force–displacement diagram illustrating thermomechanical behavior of (25%) fiber fraction shape memory polymer composites at different temperatures.

shows that the stiffness of neat SMP has been dropped by about 80% of its glassy phase stiffness when the temperature increased by 20°C from 35°C to 55°C. However, the drop in stiffness was 75% and 35% for the increase in temperature blocks 55°C–75°C and 75°C–95°C, respectively. This indicates that the major loss in material stiffness happens at the beginning of the transition region due to the commencement of the defrosting state of SMP glassy phase.

Figure 11 depicts that at 35°C, 55°C, 75°C, and 95°C, the stiffness of 20% SMPC has improved by 1, 5, 8, and 11 times, respectively, compared to neat SMP. However, the improvement in the stiffness of the 25% SMPC, as shown in Figure 12, is considerably large (1.7, 12.5, 23, and 35 times) for the same temperature levels. Obviously, the glass fiber has improved the composites' stiffness at all temperatures, which is ascribed to the high stiffness modulus of glass fibers. However, the percentage of stiffness improvement is not consistent and found to be dependent on the temperature.

Glass fiber has improved the mechanical properties of the SMPCs, although the improvement was associated with a reduction in the difference between the glassy and rubbery phases' storage moduli, which means a reduction in shape fixity ability of the material.

Thermal deformation behavior

Figures 13 and 14 depict the experimental and analytical results of both SMP and SMPC specimens under free and constrained thermal expansion conditions, respectively. The influence of reinforcement fibers on the thermal deformation behavior of the SMPCs from room temperature to above T_g is presented in Figure 13. It has been observed that fibers have dramatically changed the thermal strain behavior of the neat SMP. The neat SMP has shown positive strain at all the temperature ranges, whereas 20% SMPCs have shown positive strain at lower temperature ranges and then turn to negative strains at higher temperatures. However, 25% SMPCs have shown negative strain at all the temperature ranges.

As shown in Figure 13, the thermal strain of the SMP specimen commences at a lower temperature than the two SMPCs. This is due to high coefficient of expansion of the neat SMP compared to the SMPCs. The variation in the SMP thermal strain curve slope at low and high temperatures is shown in Figure 13, which indicates that SMP coefficient of expansion is temperature-dependent. Accordingly, the overall matrix coefficient of expansion has been calculated based on the percentage of each of the constitutive phases. Tan et al. (2014) have expressed the whole thermal strain in the SMPC as a sum of thermal strain of the fibers and the matrix phases (equation (7)). Hence, the coefficient of thermal expansion of the composite is calculated by

$$\alpha_c = \frac{\left[(1-\phi_f)\int_{T_o}^{T}\left[(1-\varphi_g(T))\alpha_r + \varphi_g(T)\alpha_g\right]dT + \phi_f\int_{T_o}^{T}\alpha_f dT\right]}{\Delta T} \tag{15}$$

Here, α_c is the thermal expansion coefficient of the composite.

The trend of the 20% SMPC sample curve has shown a positive thermal expansion at the beginning of the heating process, which has been justified in section "Modeling of 'free of load' thermal strain behavior." However, this trend has reversed, and the strain turned

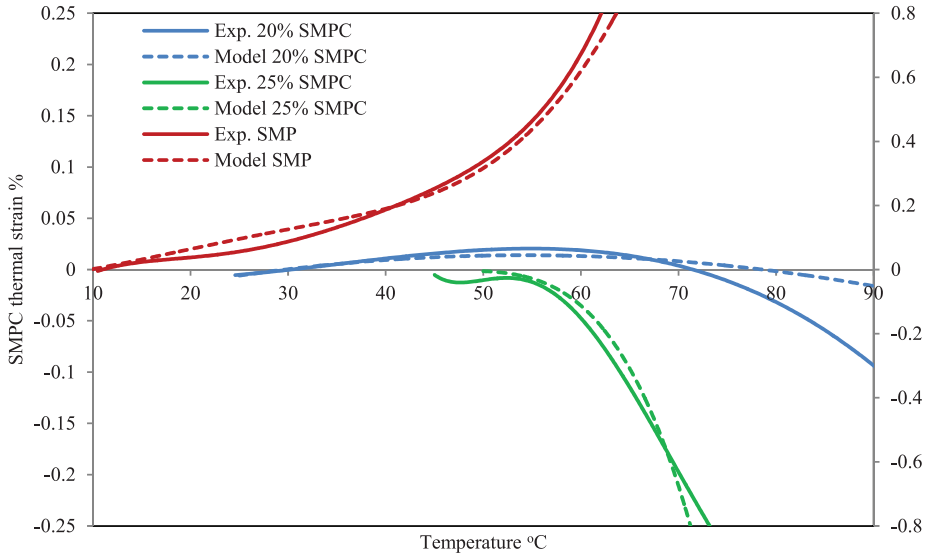

Figure 13. Experimental results and analytical model prediction of the thermal strain behavior of neat SMP and two different fiber fraction SMPCs under no-load condition.

to negative as the temperature approaches the transition region. This negative expansion behavior of the specimen is attributed to the sudden drop in the matrix modulus that makes it possible for the pre-strained fibers to retract and contract the specimen.

Due to the increase in fiber fraction of the 25% SMPC sample, the effect of the fibers on the specimen behavior becomes more dominant. Unlike the 20% specimen, there is no expansion (positive strain) happened at the beginning of the heating process. The reason for this is higher fiber fraction surpasses thermal expansion stress of the matrix that reduces compressive stress produced by the fibers. Therefore, the specimen shape remains unchanged until the inception of the transition region where the matrix modulus drops and the contraction effect of fibers increases gradually.

As the heating process is very essential in the shape programming/recovery process of parts made of SMP and SMPC, the unprecedented geometry deformation in these parts due to heating makes them inappropriate for applications that need dimensional stability.

To overcome this detrimental impact produced by the fibers on the SMPC geometry, an external tensile load during the heating process has been proposed. This tensile load intends to marginalize the fibers' effect by exerting counter stress on the fibers and ameliorates the composite geometry and dimensional stability. Indeed, the proposed applied stress has modified the way by which the thermal strain takes place in the specimens and will be shown below.

Thermal deformation behavior of the SMP and SMPC samples under tensile stress is presented in Figure 14. The behavior of SMPCs shown in Figure 14 has improved dimensional stability. The reason for this improvement is the generation of positive mechanical strain that compensates the negative strain produced by the fibers. However, there is no substantial effect of the applied stress on thermal strain behavior of SMP sample as the thermal strain is still positive, indicating that expansion takes place all the time during the heating process. Furthermore, Figure 14 still shows two slopes in the glassy and rubbery phases of the SMP curve, similar to the no applied tensile load case. For the 20% SMPC specimen, the strain starts in the positive direction and no negative strains were observed when the temperature approaches the transition region. This is because the applied tensile stress has produced positive strain and compensated negative strain.

The effect of heating on the 25% SMPC specimen's shape begins with negative strain (contraction); however, due to the applied tensile load, the shrinkage is less intensive than the stress-free case. The reason for this contraction is attributed to the drop in the matrix properties and retraction in the fibers. However, the applied stress has reduced the fiber effect, and thus the specimen geometry remains almost the same when the temperatures approach the transition region.

Figures 13 and 14 also depict the proposed analytical model results for the two considered test conditions: free of stress and constant tensile stress. Model prediction for the case where heating process is done in no stress condition is shown in Figure 13, where good correlation with the experimental results has been presented although, some discrepancies have been noticed between the model and experimental results when the tensile stress was introduced (Figure 14). This is due to the reduction in the SMP stiffness at high temperatures, and therefore some slippages have taken place between the specimen and the machine grips. On the contrary, this effect was almost negligible for the test with no applied stress because constrain-free thermal expansion was allowed in the test.

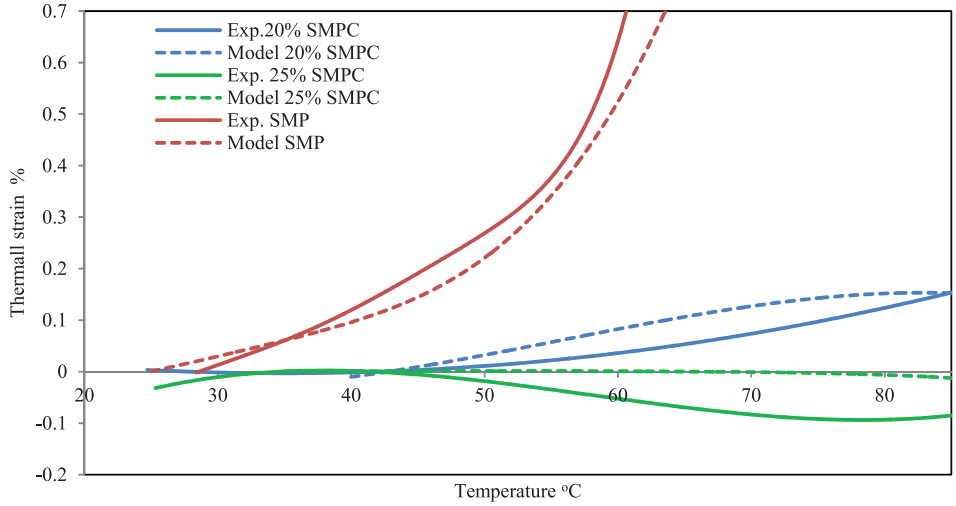

Figure 14. Experimental and analytical model prediction results of the thermal strain behavior of neat SMP and two different fiber fraction SMPCs under tensile stress. The tensile stress has changed the thermal deformation behavior and improved the shape constancy of the composites.

Conclusion

The effects of glass fiber reinforcement on the mechanical properties and the geometrical dimensional stability of the SMPC during the heating process have been investigated in this research. Initially, the mechanical and thermal properties of neat SMP and SMPCs with different glass fiber contents have been characterized using the DMA. Then, constitutive relationships have been developed to model the thermal effect on the SMPC geometrical stability.

The results revealed that below the glass transition temperature, the addition of glass fiber has improved the mechanical characteristics of the SMP. The SMPCs with 20% fiber fraction have exhibited increased storage modulus by 1.75 times the neat SMP, and for the 25% fiber fraction SMPC samples the improvement was 2.35 times. However, the improvement in the storage modulus has been found to be half of these figures at temperatures above the glass transition temperature. Furthermore, DMA results have exhibited a marginal increase in the samples' glass transition temperature from 70°C for neat SMP to 82°C and 86°C for 20% and 25% SMPCs, respectively. In contrast, the dimensional stability of the SMPC samples has been negatively affected by the inclusion of the reinforcement fibers. A noticeable deformation of SMPCs has been observed during the thermomechanical cycle due to the significant variation in the mechanical properties of the SMP between high and low temperatures and the mismatch of expansion coefficient of the fiber and the matrix. This unanticipated deformation is found to be dependent on fiber volume fraction. The 20% SMPC samples start thermal expansion at the beginning of heating cycle and turn into contraction as the temperature approaches the glass transition region. However, contraction started at the beginning of heating cycle for the 25% SMPC specimen and no expansion was observed thereafter. To overcome this unanticipated thermal deformation caused by the reinforcement fiber, a constrained heating process has been proposed by applying a constant tensile stress during heating. This technique has been found to reduce the deformity of SMPC components during the heating cycle.

Acknowledgements

The authors are indebted to the Harbin Institute of Technology, China, for providing help and material used in this work.

Declaration of conflicting interests

The author(s) declared no potential conflicts of interest with respect to the research, authorship, and/or publication of this article.

Funding

The author(s) disclosed receipt of the following financial support for the research, authorship, and/or publication of this article: The authors acknowledge the financial support provided by Iraqi Ministry of Higher Education and Scientific Research and the College of Engineering, University of Diyala, Iraq.

References

Abrahamson ER, Lake MS, Munshi NA, et al. (2003) Shape memory mechanics of an elastic memory composite resin. *Journal of Intelligent Material Systems and Structures* 14: 623–632.

Baghani M and Taheri A (2015) An analytic investigation on behavior of smart devices consisting of reinforced shape memory polymer beams. *Journal of Intelligent Material Systems and Structures* 26: 1385–1394.

Baghani M, Mohammadi H and Naghdabadi R (2014) An analytical solution for shape-memory-polymer Euler-Bernoulli beams under bending. *International Journal of Mechanical Sciences* 84: 84–90.

Beloshenko VA, Varyukhin V and Voznyak YV (2005) The shape memory effect in polymers. *Russian Chemical Reviews* 74: 265–283.

DesRoches R and Smith B (2004) Shape memory alloys in seismic resistant design and retrofit: a critical review of their potential and limitations. *Journal of Earthquake Engineering* 8: 415–429.

Fejős M, Romhany G and Karger-Kocsis J (2012) Shape memory characteristics of woven glass fibre fabric reinforced epoxy composite in flexure. *Journal of Reinforced Plastics and Composites* 31: 1532–1537.

Gunes IS and Jana SC (2008) Shape memory polymers and their nanocomposites: a review of science and technology of new multifunctional materials. *Journal of Nanoscience and Nanotechnology* 8: 1616–1637.

Hahn HT (1976) Residual stresses in polymer matrix composite laminates. *Journal of Composite Materials* 10: 266–278.

Han DZQ, Fan MM, et al. (2012) pH-induced shape-memory polymers. *Macromolecular Rapid Communications* 33: 1055–1060.

Ivens J, Urbanus M and De Smet C (2011) Shape recovery in a thermoset shape memory polymer and its fabric-reinforced composites. *Express Polymer Letters* 5: 254–261.

Ji F, Zhu Y, Hu J, et al. (2006) Smart polymer fibers with shape memory effect. *Smart Materials and Structures* 15: 1547.

Keller PN, Lake MS, Francis W, et al. (2004) Development of a deployable boom for microsatellites using elastic memory composite material. In: *45th AIAA/ASME/ASCE/AHS/ASC structures, structural dynamics & materials conference*, Palm Springs, CA, 19–22 April.

Lan X, Liu Y, Lv H, et al. (2009) Fiber reinforced shape-memory polymer composite and its application in a deployable hinge. *Smart Materials and Structures* 18: 024002.

Lendlein A and Kelch S (2002) Shape-memory polymers. *Angewandte Chemie International Edition* 41: 2034–2057.

Lendlein A, Jiang H, Jünger O, et al. (2005) Light-induced shape-memory polymers. *Nature* 434: 879–882.

Leng J, Lan X, Liu Y, et al. (2011) Shape-memory polymers and their composites: stimulus methods and applications. *Progress in Materials Science* 56: 1077–1135.

Leng J, Lv H, Liu Y, et al. (2007) Electroactivate shape-memory polymer filled with nanocarbon particles and short carbon fibers. *Applied Physics Letters* 91: 144105.

Liu Y, Du H, Liu L, et al. (2014) Shape memory polymers and their composites in aerospace applications: a review. *Smart Materials and Structures* 23: 023001.

Liu Y, Dunn ML and McCluskey P (2003) Thermomechanical recovery couplings of shape memory polymers in flexure. *Smart Materials and Structures* 12: 947–954.

Liu Y, Gall K, Dunn ML, et al. (2006) Thermomechanics of shape memory polymers: uniaxial experiments and constitutive modeling. *International Journal of Plasticity* 22: 279–313.

Liu Y, Lv H, Lan X, et al. (2009) Review of electro-active shape-memory polymer composite. *Composites Science and Technology* 69: 2064–2068.

Lu H, Yu K, Sun S, et al. (2010) Mechanical and shape-memory behavior of shape-memory polymer composites with hybrid fillers. *Polymer International* 59: 766–771.

Manders PW and Bader MG (1981) The strength of hybrid glass/carbon fibre composites. *Journal of Materials Science* 16: 2233–2245.

Nairn JA and Zoller P (1985) Matrix solidification and the resulting residual thermal stresses in composites. *Journal of Materials Science* 20: 355–367.

Nishikawa M, Wakatsuki K, Yoshimura A, et al. (2012) Effect of fiber arrangement on shape fixity and shape recovery in thermally activated shape memory polymer-based composites. *Composites Part A: Applied Science and Manufacturing* 43: 165–173.

Ohki T, Ni Q-Q, Ohsako N, et al. (2004) Mechanical and shape memory behavior of composites with shape memory polymer. *Composites Part A: Applied Science and Manufacturing* 35: 1065–1073.

Ratna D and Karger-Kocsis J (2008) Recent advances in shape memory polymers and composites: a review. *Journal of Materials Science* 43: 254–269.

Ray B (2004) Thermal shock on interfacial adhesion of thermally conditioned glass fiber/epoxy composites. *Materials Letters* 58: 2175–2177.

Razzaq MY and Frormann L (2007) Thermomechanical studies of aluminum nitride filled shape memory polymer composites. *Polymer Composites* 28: 287–293.

Sahoo NG, Jung YC, Goo NS, et al. (2005) Conducting shape memory polyurethane-polypyrrole composites for an electroactive actuator. *Macromolecular Materials and Engineering* 290: 1049–1055.

Sahoo NG, Jung YC, Yoo HJ, et al. (2007) Influence of carbon nanotubes and polypyrrole on the thermal, mechanical and electroactive shape-memory properties of polyurethane nanocomposites. *Composites Science and Technology* 67: 1920–1929.

Schmidt AM (2006) Electromagnetic activation of shape memory polymer networks containing magnetic nanoparticles. *Macromolecular Rapid Communications* 27: 1168–1172.

Tan Q, Liu L, Liu Y, et al. (2014) Thermal mechanical constitutive model of fiber reinforced shape memory polymer composite: based on bridging model. *Composites Part A: Applied Science and Manufacturing* 64: 132–138.

Vedula M, Pangborn RN and Queeney RA (1988) Modification of residual thermal stress in a metal-matrix composite with the use of a tailored interfacial region. *Composites* 19: 133–137.

Xu W and Li G (2010) Constitutive modeling of shape memory polymer based self-healing syntactic foam. *International Journal of Solids and Structures* 47: 1306–1316.

Yang B, Min Huang W, Li C, et al. (2005) Effects of moisture on the glass transition temperature of polyurethane shape memory polymer filled with nano-carbon powder. *European Polymer Journal* 41: 1123–1128.

Zhou B, Liu Y-J, Lan X, et al. (2009) A glass transition model for shape memory polymer and its composite. *International Journal of Modern Physics B: Condensed Matter Physics, Statistical Physics, Applied Physics* 23: 1248–1253.